Chem

CellPress

Article

Cross-reactive binding versus selective phosphate sensing in an imine macrocycle sensor

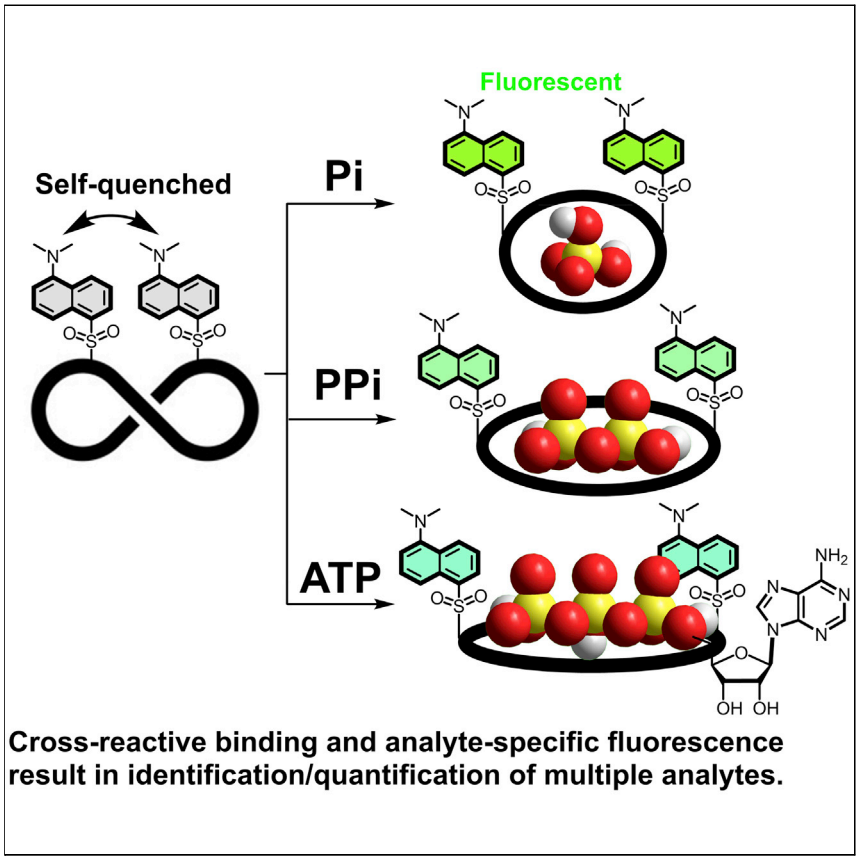

Cross-reactive binding and analyte-specific fluorescence result in identification/quantification of multiple analytes.

A selective sensing of multiple phosphate analytes and their mixtures is achieved using a single fluorescent sensor comprising a cross-reactive (i.e., non-selective) receptor that binds various phosphates and an environmentally sensitive fluorophore that yields an analyte-selective response.Such a sensor allows for a simplified sensing of multiple analytes including phosphates and may find application in monitoring phosphorylation processes of biological and pharmaceutical assays.

Aco Radujević, Andrej Penavic, Radoslav Z. Pavlović, Jovica D. Badjić, Pavel Anzenbacher, Jr.

pavel@bgsu.edu

Highlights

New fluorescent sensor based on a cross-reactive aliphatic imine receptor was studied

Environmentally sensitive fluorophore was used to obtain analyte-selective responses

A single chemosensor is capable of identification/quantification of multiple analytes

A single chemosensor recognizes phosphates (ATP, ADP, AMP, PPi, and Pi) in their mixtures

Radujević et al., Chem 8, 1–17
August 11, 2022
https://doi.org/10.1016/j.chempr.2022.05.010

Please cite this article in press as: Radujević et al., Cross-reactive binding versus selective phosphate sensing in an imine macrocycle sensor, Chem (2022), https://doi.org/10.1016/j.chempr.2022.05.010

Chem

CellPress

Article

Cross-reactive binding versus selective phosphate sensing in an imine macrocycle sensor

Aco Radujević,[1] Andrej Penavic,[1] Radoslav Z. Pavlović,[2] Jovica D. Badjić,[2] and Pavel Anzenbacher, Jr.[1,3,*]

SUMMARY

We demonstrate a new approach to chemosensors suited for analysis of phosphate mixtures. Here, a combination of a cross-reactive receptor and an environmentally sensitive fluorophore allows for binding various phosphates and obtaining analyte-specific fluorescence response. We have investigated a flexible and cross-reactive imine-pyrrole macrocycle comprising both hydrogen-bond donors and acceptors, one that is capable of self-organizing in response to phosphate-type anions. This cross-reactive binding was elucidated by theoretical and nuclear magnetic resonance (NMR) studies. Incorporating an environmentally sensitive dansyl fluorophore, which responds to the presence of analytes with a varying degree of fluorescence amplification, resulted in translating the cross-reactive binding into variable analyte response and enabled differentiation of oxyanions. The trend of anion affinities is $H_2PO_4^-$>AMP>$H_2P_2O7^{2-}$>ADP>ATP. We show that only one sensor can differentiate among various phosphates including their mixtures. By applying machine learning algorithms, we were able to differentiate between 12 anions and accurately quantify ATP, ADP, AMP, PPi, Pi, and their mixtures.

INTRODUCTION

In the past, the paradigm for the design of artificial receptors and sensors was the lock and key concept utilizing preorganized receptors that associate with a substrate or analyte in a specific fashion to achieve selective recognition.[1] This approach, while appropriate for analytes of strategic importance, suffers from disadvantages such as a slow on-off rate, high cost of synthesis, and is often hampered by a partial cross-reactivity.[2] Perhaps most importantly, the lock and key approach is limited to one type of sensor for one type of analyte. Driven largely by the interest in complex analytes, the focus in molecular sensing is shifting from selective sensors toward cross-reactive sensors that are not selective and employ recognition of a response pattern[3–6] as it is in so-called chemical noses,[7–9] tongues,[10–12] etc. Such sensors then utilize cross-reactive recognition elements to identify an analyte based on the response pattern that originates from a number of nonselective sensors.[4,13–17] Conventional wisdom holds that cross-reactive sensor arrays, because of the "lower recognition quality (specificity)" of the sensors, should be composed of a large number of such array elements. To mitigate the potential problems associated with large datasets, redundancy, and a low signal-to-noise ratio, a new approach of a rational design of the arrays that allows for minimizing the number of the array elements came to the forefront.[18,19] This has been demonstrated on optical sensor arrays

The bigger picture

Phosphates play important roles in nature and biotechnology. Their structures range from orthophosphate to nucleotide mono-, di-, or triphosphates. The structural diversity, various protonated states, and hydrates make designing selective sensors difficult. Here, the selective (key & lock) sensors are frequently failing. Thus, sensor arrays (chemical noses or tongues) comprising multiple cross-reactive sensors while providing a fingerprint-like response are an important advance. However, sensor arrays require multiple sensors, which necessitates recording large datasets rendering subsequent analysis cumbersome. We show that this may be overcome by a new type of sensors capable of cross-reactive sampling of many analyzed species while providing an analyte-specific response, thereby allowing for simplified sensing of multiple analytes including phosphates. Such sensors may find application in monitoring phosphorylation processes in corresponding biological and pharmaceutical assays.

Please cite this article in press as: Radujević et al., Cross-reactive binding versus selective phosphate sensing in an imine macrocycle sensor, Chem (2022), https://doi.org/10.1016/j.chempr.2022.05.010

where a careful array optimization, aimed to eliminate redundant information and improve discrimination accuracy, was performed.[18,20–22] From the chemistry perspective, this has been partly addressed, for example, by increasing the multiplicity of the outputs in receptors carrying multiple chromophores.[23–26] Thus, the pendulum swings back toward the arrays that comprise the smallest possible number of sensor elements. In an extreme, one could consider a single sensor element that would comprise a cross-reactive (non-selective) receptor capable of reversible binding-and-reporting on (sampling) multiple analyte components and a signaling device (chromophore) capable of rendering an analyte-specific information.[27–29] Such an approach, if successful, would be particularly valuable for analytes for which the selective receptors are difficult to design and synthesize. We reasoned that such difficult to analyze analytes are anions, and phosphates in particular.

Phosphate anions are ubiquitous in nature[30] and living organisms[31] and used in industry and agriculture. Their use as fertilizers[32] frequently results in anthropogenic eutrophication, the ecological transformation of water bodies by nutrient pollution.[33]

There are many methods for determination of phosphate (orthophosphate, Pi) starting from phosphomolybdate methods for determination of orthophosphate.[34,35] Other methods that rely on electrochemistry[36,37] or field-effect transistors[38,39] are being pursued. Although some of these methods are useful for orthophosphate analysis, the current trends, particularly in biochemistry and biology, are focusing on the analyses of phosphate esters and anhydrides such as nucleotide phosphates and their mixtures.[40] This is because the phosphates and particularly the biological phosphates usually occur in mixtures, and their analysis requires advanced instrumental methods such as ion chromatography for the nucleobase-free phosphates[41] and reverse-phase HPLC for nucleotide phosphates.[42,43] Despite many advantages, these methods for analyzing phosphate mixtures require expensive instrumentation, highly skilled personnel and time, and are therefore not amenable to high-throughput or field applications. In the realm of molecular biology, commercial tests have been developed that employ multiple enzyme assays. Such assays, however, require strictly controlled environment (pH, temperature, and additives/buffers) and traditionally have a relatively low shelf-life. Thus, a chemically stable single-molecule sensor for multiple phosphates would be a boon in the situations where a rapid high-throughput method for sensing of multiphosphate mixtures is desired.

Current reviews[44–46] show that supramolecular chemistry studies of synthetic receptors and sensors made progress in the area of recognition of phosphate-type anions and is starting to produce methods for analysis of phosphates. However, there are still obstacles associated with extensive hydration,[47] protonation equilibria, and the structural diversity of phosphate anions that make the design and utilization of phosphate receptors difficult.[48,49] Thus, sensors for anions that are capable of distinguishing and quantifying phosphates such as (di)hydrogen phosphate (Pi), pyrophosphate (PPi), as well as nucleotide triphosphates, diphosphates, and monophosphates as markers of metabolic processes[50,51] in water while providing a clearly observable turn-ON signal are still being sought.[48,52–55]

In the design of our sensor, we decided to employ a cross-reactive receptor to bring many different analytes close to the signaling fluorophore. Then, we decided to use a fluorophore that displays a significant charge transfer (ICT) in the excited state, which is sensitive to differences in charge density/polarity in its close vicinity. Our hypothesis is that the cross-reactive receptor will bind and release (sampling) various

[1]Department of Chemistry, Bowling Green State University, Bowling Green, OH 43403, USA

[2]Department of Chemistry and Biochemistry, Ohio State University, Columbus, OH 43210, USA

[3]Lead contact

*Correspondence: pavel@bgsu.edu

https://doi.org/10.1016/j.chempr.2022.05.010

Please cite this article in press as: Radujević et al., Cross-reactive binding versus selective phosphate sensing in an imine macrocycle sensor, Chem (2022), https://doi.org/10.1016/j.chempr.2022.05.010

phosphate analytes while displaying a different response to different phosphates (analyte-specific signal). Thus, we will have cross-reactive binding, but superimposed on this is the analyte-specific response (reporting). The result is a selective sensing of multiple analytes. To examine the above concept of analysis of difficult-to-address analytes using a single cross-reactive receptor combined with a chromophore capable of generating analyte-specific information, we decided to investigate a large and flexible macrocyclic receptor to be modified with an environmentally sensitive dansyl fluorophore that due to its ICT nature of the excited state,[56] it yields a differential response to various anions based on their size, flexibility, hydrogen-bonding patterns, surface charge density, and other factors.[57–59] As a receptor, we selected a macrocyclic oligopyrrole imine-based macrocycles deemed to be attractive because of its hydrogen-bond (HB) properties, both as donors (pyrrole) and acceptors (imine) of HBs, as well as their high conformational flexibility for complementing potential guests,[60–62] including anions.[63] Schiff bases were used as ligands for various metal ions,[64–66] as well as for binding of anions,[67–73] and are therefore a suitable platform for the proposed phosphate sensor.

RESULTS AND DISCUSSION

Design and synthesis of fluorescent imine macrocycles

In the design of the sensor, the important consideration is the flexibility of the receptor. The following paragraphs will reveal how the flexible imine macrocycle receptor (guest) based on aliphatic imine moieties fluidly adapts to the demands of multiple guests. In essence, we abdicated the preorganization for self-organization in the presence of a guest. This feature is then complemented by the use of an environmentally sensitive fluorophore that makes it possible to extract analyte-specific fluorescence information from only one sensor molecule.

To explore the above concept, we have prepared imine macrocycles using dipyrromethane dialdehyde **1**[74] and aliphatic diamine **2**[75] (Scheme 1; see Scheme S1 in supplemental experimental procedures). Reacting precursors **1** and **2** in an equimolar ratio under a high dilution resulted in a predominant formation of macrocyclic products **3** and **4** (Scheme 1; Figures S2 and S9). After several recrystallization steps, we were able to isolate pure **3**, which was characterized by 1D (^{1}H, ^{13}C), 2D (COSY, ROESY, HSQC, HMBC, and DOSY) nuclear magnetic resonance (NMR) spectroscopic methods and high-resolution MALDI TOF spectrometry (Figures S18–S27).

The low yield of product **3** (3 % after three recrystallizations) led us to employing templated synthesis of **3**. Given the propensity of the pyrrole moieties to bind to anions, we decided to probe anionic templates including chloride, dihydrogen phosphate, and pyrophosphate. Here, in the case of dihydrogen phosphate and pyrophosphate, we observed a templated formation of **3** (the desired 2 + 2 product) at the expense of linear oligomers while the formation of large 3 + 3 product was not observed (Figures S14–S16). On the other hand, we have not observed the same templating effect in the case of chloride. To further explore the binding of phosphate and pyrophosphate by **3**, we decided to examine its conformational characteristics—first, in the resting state, and then, in the presence of anionic guests. Thus, Monte-Carlo conformational search[76,77] (MTLMOD, OPLS3e force field[78]) of **3** gave 633 lowest energy conformers (10 kcal/mol of steric energy), which were further optimized via a semiempirical method (PM6) followed by density functional theory (DFT) calculations (B3LYP/6-31G+[2d], with implicit DMSO solvation). The lowest energy conformer was subjected to frequency calculations showing the absence of any imaginary frequencies. Based on the computational work, the

Please cite this article in press as: Radujević et al., Cross-reactive binding versus selective phosphate sensing in an imine macrocycle sensor, Chem (2022), https://doi.org/10.1016/j.chempr.2022.05.010

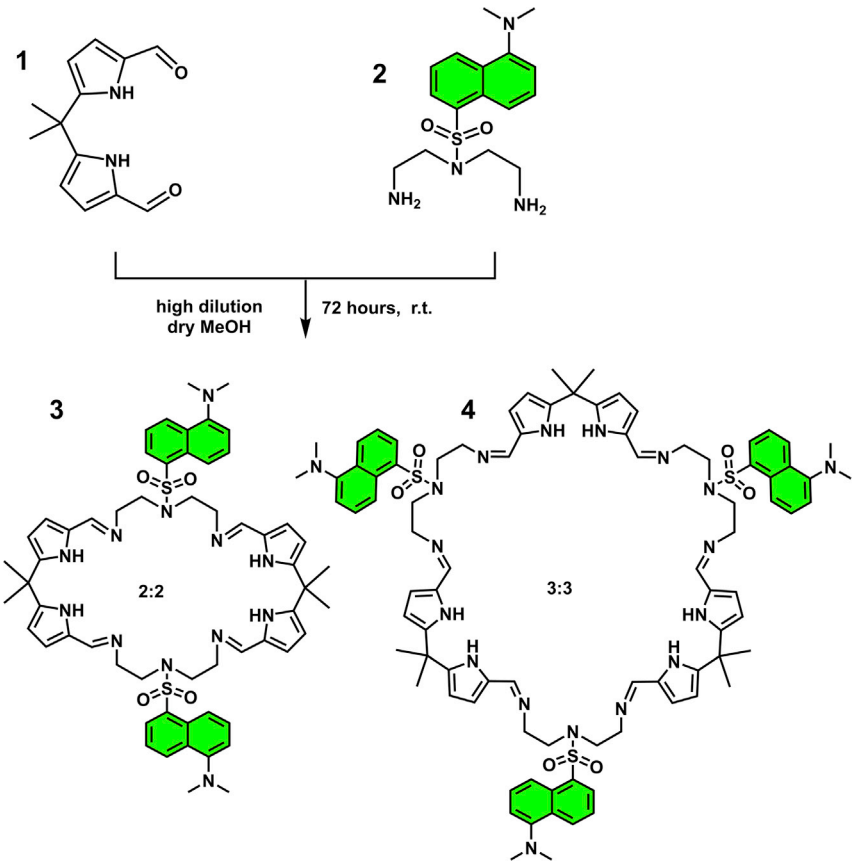

Scheme 1. Synthesis of macrocycle 3

Dipyrromethane dialdehyde **1** and diamine **2** were mixed in an equimolar ratio under high-dilution conditions (in MeOH) to obtain two major macrocycles- [2+2] macrocycle **3** and [3+3] macrocycle.

macrocycle **3** predominantly populates the equilibrium (75% from the Boltzmann distribution) in its folded and C_1 symmetric form (Figure 1B). This folded conformation was confirmed by ^{1}H-^{1}H ROESY NMR spectroscopy (for details on the structure of the receptor, see Figures S21 and S22). In the later paragraphs, we show that this folded conformation of **3** is capable of unfolding to adapt to the structural demands of the anionic guests and that this process is also accompanied by the significant change in the fluorescence response.

NMR solution studies of sensor 3 and $TBAH_2PO_4$

After an incremental addition of tetrabutylammonium dihydrogen phosphate ($TBAH_2PO_4$) to the sensor **3** (Figure 2A; see also Figures S41 and S42), the ^{1}H NMR resonances from the pyrrolic **NH** underwent a considerable downfield shift from 10.9 to 13.5 ppm as a result of pyrrolic **NH** protons being engaged in hydrogen bonding with the phosphate guest. Concurrently, the imine **N=C-H$_g$** hydrogens became broadened and magnetically deshielded (Figure 2B) as a result of an unfolding of macrocycle **3** upon binding of the anionic guest (see below). We hypothesize that the broadening of **H$_g$** is related to (1) a reduction in the conformation mobility of this part of the molecule causing a faster relaxation of its nuclei and (2) protonation of the imine functionality occurring on intermediate NMR timescale. In fact, the complexation of $H_2PO_4^-$ by an imine-type host followed by anion-to-host proton transfer was previously described.[71] When the addition of $H_2PO_4^-$ to **3** was monitored with ^{31}P NMR spectroscopy (Figure S34), a large magnetic perturbation of

Please cite this article in press as: Radujević et al., Cross-reactive binding versus selective phosphate sensing in an imine macrocycle sensor, Chem (2022), https://doi.org/10.1016/j.chempr.2022.05.010

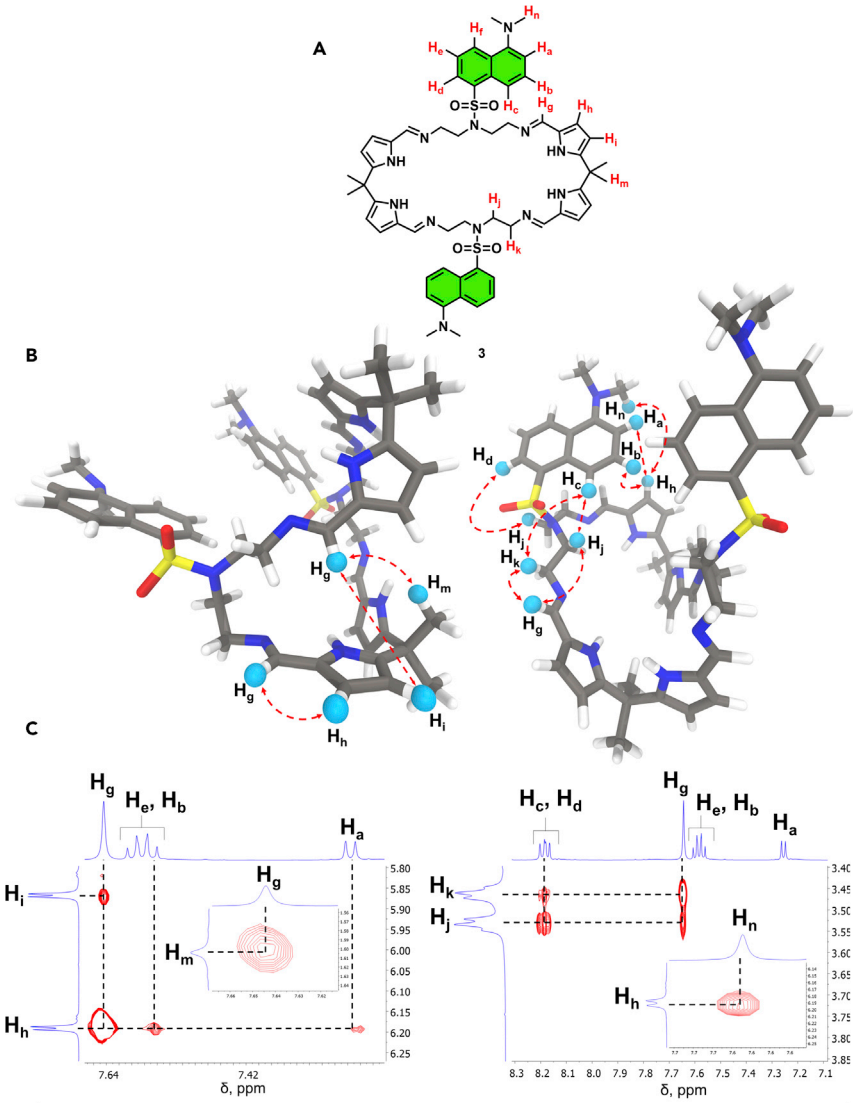

Correlated hydrogens	H_g-H_h	H_g-H_i	H_g-H_m	H_g-H_k	H_g-H_j	H_d-H_j	H_c-H_j	H_c-H_k	H_n-H_h	H_a-H_h	H_b-H_h
Distance (Å)	2.8	4.5	3.7	2.2	3.6	3.1	2.4	4.5	4.5	4.4	4.2

Figure 1. Fluorescent macrocyclic sensor 3 used in this study

(A) Molecular structure of the receptor **3** (left).

(B) DFT optimized geometry of receptor 3 (two different perspectives) showing a partially twisted conformation of the receptor in the resting state. Red arrows indicate NOE contacts between highlighted hydrogens.

(C) Selected regions of 2D ^{1}H-^{1}H ROESY NMR spectra (500 MHz, DMSO-d_6 at 298 K) of receptor 3 (3.0 mM solution) displaying important cross-peaks correlations between different segments of the molecule emphasizing partially twisted conformation of the receptor in the resting state (top). Distance (Å) between highlighted hydrogens is depicted in the table (bottom).

the resonance from the phosphorus in $H_2PO_4^-$ ($\Delta\delta$ = 1.50 ppm) indicated the anion forming HBs with **3**.

To gain further insight into the binding mode of phosphate, we performed ^{1}H-^{1}H ROESY NMR spectroscopic measurements of **3** in DMSO-d_6 in the presence of an excess of $H_2PO_4^-$ (Figure 3B; see Figures S29 and S30). The principal ROE

Please cite this article in press as: Radujević et al., Cross-reactive binding versus selective phosphate sensing in an imine macrocycle sensor, Chem (2022), https://doi.org/10.1016/j.chempr.2022.05.010

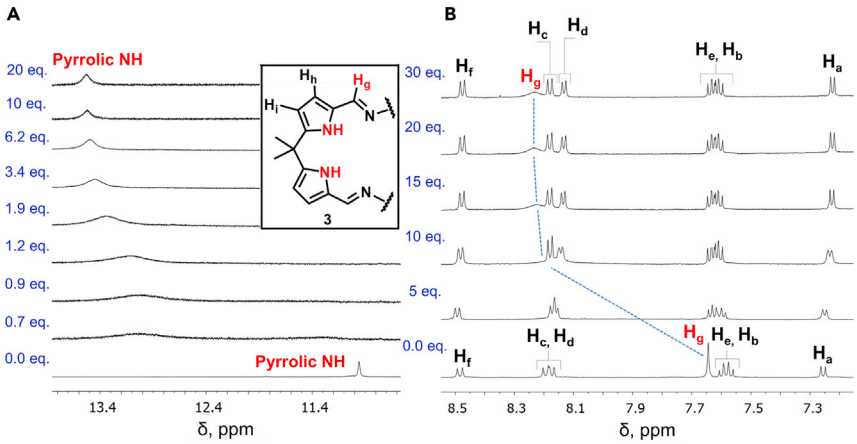

Figure 2. 1H NMR titration experiment of receptor 3 with $TBAH_2PO_4$

(A) Pyrrolic **NH** and B: dansyl and imine **N=C-Hg** region of ^{1}H NMR (500 MHz, DMSO-d_6 at 298 K) spectra measured upon addition of increasing amount of $TBAH_2PO_4$ to the host **3** (5.65 mM).

correlations are highlighted in Figure 3B, whereas the energy-minimized structure (DFT) of the binary complex in Figure 3A depicts the pertinent contacts in space. In particular, the magnetization transfer between $H_g \leftrightarrow H_h$ and $H_g \leftrightarrow H_k$ indicates syn-relationship of these groups. The cross signals between H_c and H_d from the dansyl unit with H_k and H_j within the macrocycle are commensurate with their proximity (Figure 3B). Indeed, DFT optimized geometry of $H_2PO_4^-$ docked within **3** and forming hydrogen bonds with its pyrroles (Figure 3A) showed a conformation of the host in which all the ROE contacts are within 5 Å. It follows that receptor **3** has to unfold to accommodate the phosphate anion: although pyrroles and imine nitrogens move in space to complement the HB sites in the guest, the dansyl groups remain at top of the cleft. Taken together, these observations highlight the critical conformational flexibility of the macrocyclic sensor 3.

NMR solution studies of sensor 3 and $(TBA)_3HP_2O_7$

The capacity of **3** to accommodate the phosphate anions by changing shape was further studied with the larger pyrophosphate. As in the case of phosphate, ^{1}H NMR spectroscopic titration of $HP_2O_7^{3-}$ to **3** (Figure S43) showed a downfield shift of the pyrrolic **NH** resonance ($\Delta\delta$ = 3.33 ppm, Figure 4B), suggesting a strong hydrogen bonding between the **N-H** and the $HP_2O_7^{3-}$. Further, a large downfield shift of the positively polarized **N=C-Hg** protons ($\Delta\delta$ = 1.0 ppm, Figure 4B) suggests the host-guest HB interaction as well. DFT energy-minimized geometry, and the corresponding hydrogen bonds are highlighted in Figure 4A. Interestingly, a complex behavior of the sensor **3** in the presence of $HP_2O_7^{3-}$ (Figure S43) indicated the formation of higher order complexes. We reasoned that at the beginning of the titration, when **3** was in excess, the pyrophosphate termini could be engaged in separate binding events to hold onto two hosts. With an excess of pyrophosphate although, such ternary complex appears to rearrange to form the final 1:1 complex. This hypothesis is in line with fluorescence titration studies performed at lower concentration of the receptor **3** (see Figure 5C).

To probe the conformation of $[HP_2O_7 \subset 3]^{3-}$, we completed a series of NMR spectroscopic measurements (COSY, NOESY, HSQC, and ESI-MS, see Figures S36–S40) with an excess of pyrophosphate to ensure the predominant formation of the binary complex. The absence of NOE cross-peaks between naphthalene hydrogens and

Please cite this article in press as: Radujević et al., Cross-reactive binding versus selective phosphate sensing in an imine macrocycle sensor, Chem (2022), https://doi.org/10.1016/j.chempr.2022.05.010

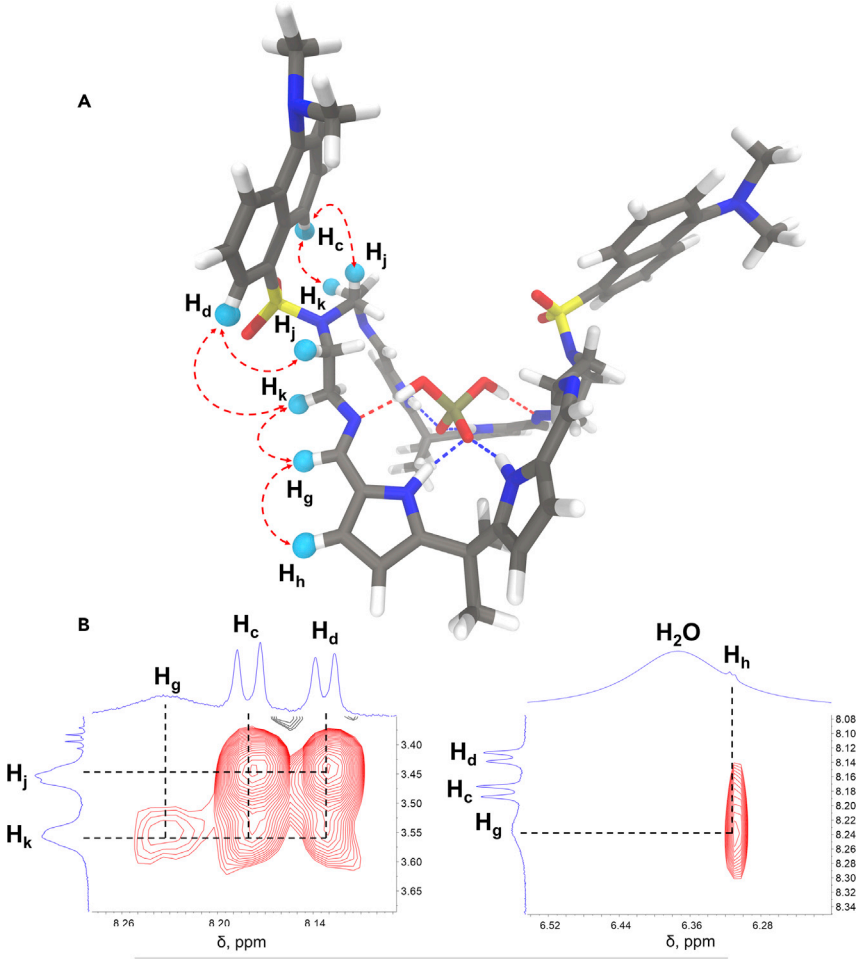

Correlated hydrogens	H_g-H_h	H_g-H_k	H_c-H_j	H_d-H_j	H_c-H_k	H_d-H_k
Distance (Å)	2.8	2.2	2.4	2.4	4.5	4.5

Figure 3. Binary $[H_2PO_4 \subset 3]^-$ complex

(A and B) (A) DFT optimized geometry (B3LYP: 6-31G+(2d)) of binary $[H_2PO_4 \subset 3]^-$.complex; (B) Selected regions of ^{1}H-^{1}H ROESY 2D NMR (500 MHz, DMSO-d_6 at 298 K) spectrum of **3** (5.65 mM) and an excess of $TBAH_2PO_4$. Distances (Å) between hydrogen nuclei showing ROEs were obtained from the energy-minimized structure of the complex.

the macrocyclic core suggested an outward orientation of the dansyl groups (Figure S37). The lack of NOE cross-correlation between imine N=C-H_g and β-pyrrolic H_h is in line with their anticonfiguration. Finally, the transfer of magnetization between $H_g \leftrightarrow H_k \leftrightarrow H_j$ corroborated their syn-relationship. A synergistic participation of the pyrrole NH and imine N=C-H_g protons in hydrogen bonding was considered in docking the pyrophosphate within **3** for energy minimization by DFT (Figure 4A). Taken together, the formation of the complex between **3** and the larger $HP_2O_7^{3-}$ results in a fully occupied binding pocket as well in complete unwinding of the macrocyclic receptor with wide separation of the dansyl moieties.

The ^{1}H DOSY NMR measurements (Figures S26, S33, and S39) suggest that conformational unfolding and increase in the apparent size of the receptor was gradual and correlated with the size of the guest. Thus, apo **3** showed hydrodynamic radius of

Please cite this article in press as: Radujević et al., Cross-reactive binding versus selective phosphate sensing in an imine macrocycle sensor, Chem (2022), https://doi.org/10.1016/j.chempr.2022.05.010

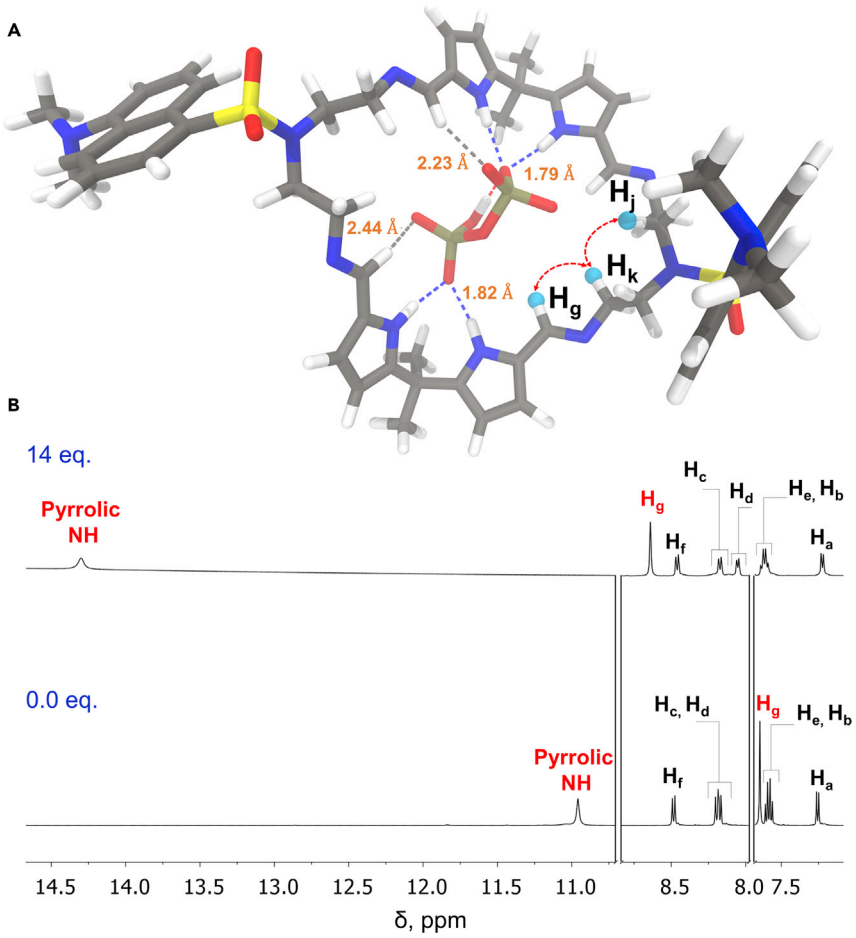

Figure 4. Binary $[HP_2O_7 \subset 3]^{3-}$ complex

(A) DFT optimized geometry (B3LYP: 6-31G + [2d]) of binary $[HP_2O_7 \subset 3]^{3-}$complex.

(B) Selected regions of ^{1}H NMR (500 MHz, DMSO-d_6 at 298 K) spectra of **3** (2.56 mM) in the free (bottom) and bound (top) state (14 equiv of $(TBA)_3HP_2O_7$).

r_H = 8.4 Å, whereas the phosphate- and pyrophosphate-bound receptors showed r_H = 9.7 Å and r_H = 10.7 Å, respectively. This correlates well with the DFT calculated radii of 8.7, 9.4, and 11.3 Å, respectively.

Absorption and fluorescence titration studies

Clearly, the sensor **3** shows conformational flexibility and an ability to recognize and accommodate oxo-anions, a feature that could be advantageous for sensing. The conformational changes observed in the NMR spectra are reflected by changes in the optical properties of the environmentally sensitive dansyl fluorophore in an analyte-specific fashion that can be observed using UV-vis and fluorescence spectroscopy. In the UV-vis spectra, we observe the charge transfer maximum of the dansyl chromophore at 343 nm, which shows a decrease in absorbance and appearance of a clearly defined isosbestic points (Figures S44–S48) upon addition of anions. Because **3** is stable in DMSO-water solutions, at least up to 20% (v/v), we performed the anion-sensing experiments with purely aqueous solutions of anions while the concentration of water in DMSO was constant at 15% (Figures S49–S52). The sensing experiments were then performed by recording the anion-induced changes in the fluorescence spectra. For example, the presence of sodium dihydrogen phosphate

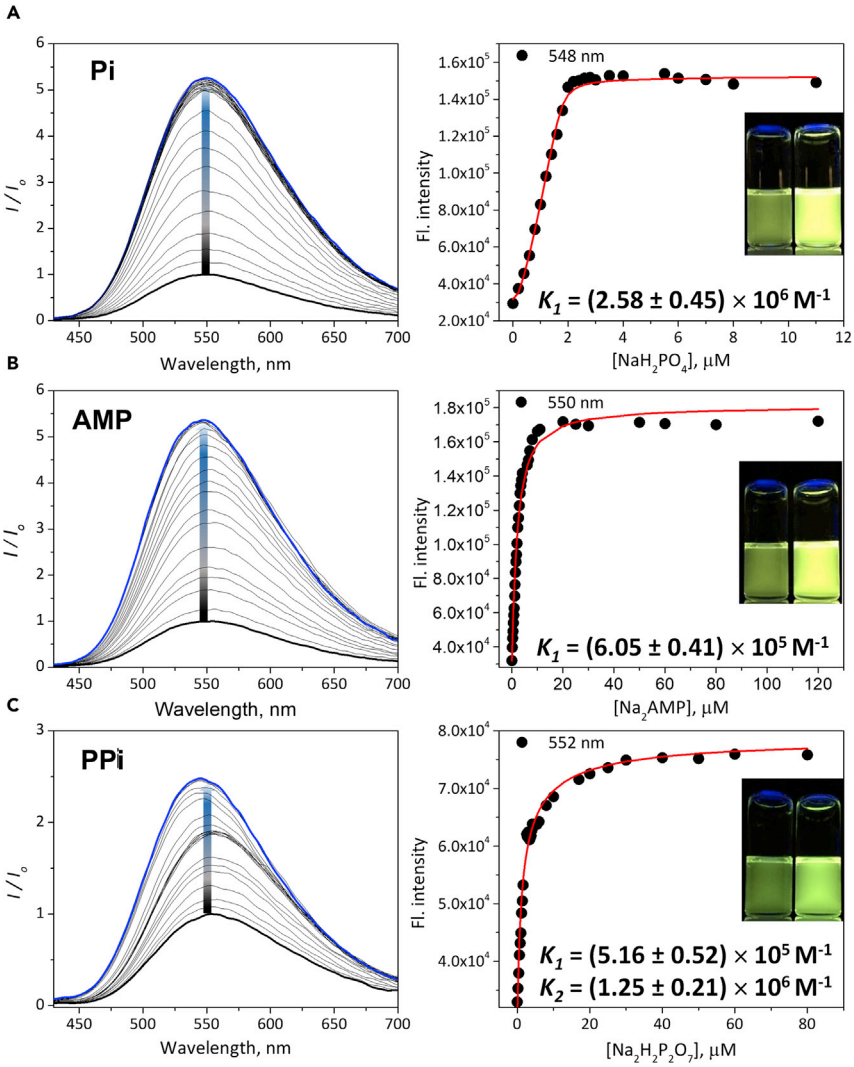

Figure 5. Fluorescence titration studies of the fluorescent probe 3 with Pi, AMP, and PPI

(A– C) Fluorescence titration of **3** (1 x 10^{-6} M) upon incremental addition of (A) NaH_2PO_4, λexc = 319 nm; (B) Na_2AMP, λexc = 319 nm; and (C) $Na_2H_2P_2O_7$, λexc = 395 nm in 15 % water in DMSO (DMSO: water = 85:15 v/v). A nonlinear least-square analysis of the binding isotherms was used to calculate the binding constants.

yielded ca. 6-fold fluorescence amplification (Figure 5A). This behavior is in line with the environmentally sensitive nature of the dansyl chromophore.[57] Importantly, the utility of **3** as a potential sensor for anions is augmented by the notable fluorescence enhancement in the presence of strongly bound anions. This is a consequence of rigidification of **3** in the complex with anion, which dramatically limits self-quenching and rotational and vibrational motions of the dansyl fluorophore in the complex compared with the free state.[79] Thus, deactivation of the excited state through non-radiative decay is suppressed, resulting in an increase of the fluorescence intensity.

A number of anionic analytes in the form of their sodium salts in water were explored, including halides (F^-, Cl^-, Br^-, and I^-), oxo-anions ($H_2PO_4^-$, $H_2P_2O_7^{2-}$, HSO_4^-, NO_3^-, and $HAsO_4^{2-}$), as well as biological phosphates (AMP, ADP, and ATP). Their affinity constants were calculated (Table 1), and limits of detection/quantitation

Please cite this article in press as: Radujević et al., Cross-reactive binding versus selective phosphate sensing in an imine macrocycle sensor, Chem (2022), https://doi.org/10.1016/j.chempr.2022.05.010

Table 1. Binding constants (K_a, M^{-1})[a] calculated for 3 and the anionic analytes in 15% water in DMSO

Anion	Binding constant	Amplification (%)
Cl^-	NR [b]	0
Br^-	NR [b]	0
I^-	NR [b]	0
F^-	$K_1 = (4.13 \pm 0.76) \times 10^4$ $K_2 = (9.45 \pm 0.20) \times 10^2$	46
$H_2PO_4^-$	$(2.58 \pm 0.45) \times 10^6$	426
$H_2P_2O_7^{2-}$	$K_1 = (5.16 \pm 0.52) \times 10^5$ $K_2 = (1.25 \pm 0.21) \times 10^6$	148
$HAsO_4^{2-}$	$(3.55 \pm 0.57) \times 10^6$	664
HSO_4^-	NR [b]	0
NO_3^-	NR [b]	0
AMP	$(6.05 \pm 0.41) \times 10^5$	437
ADP	$(5.29 \pm 0.63) \times 10^5$	99
ATP	$(1.39 \pm 0.18) \times 10^5$	57

[a]The K_a values were calculated based on the change in fluorescence intensity upon an incremental addition of each anion in the form of their sodium salts. Excitation wavelengths were selected using isosbestic points (obtained from UV-vis titrations) or at the minimum change of absorbance. The association constants were calculated using non-linear least-square fitting. Corresponding random distribution of the residuals is shown in supplemental information proving the fidelity of the fittings.
[b]No appreciable response was observed.

(LOD/LOQ) were determined (Table S1). The LODs are generally below 1 μM, which compares favorably with many sensors in the literature.[45] With the exception of fluoride and PPi at lower PPi concentration, the stoichiometry of the complexes was 1:1. Hence, 1:1 model fitting was used to calculate the affinity constants. The only different biding pattern we observed was for PPi. As seen from the UV-vis, fluorescence, and NMR titrations, at the beginning of the titration, when the concentration of the sensor **3** is larger than the concentration of the PPi, a 2:1 (sensor:PPi) complex appears to be formed. This is evidenced by the less defined isosbestic point in the UV-vis spectra (Figure S47) and the fitting of the isotherm obtained from the fluorescence titrations (Figure 5C) according to the 2:1 binding model.[80,81] The interaction between sensor **3** and PPi is reflected by high binding constants ($K_1 = [5.16 \pm 0.52] \times 10^5\ M^{-1}$ and $K_2 = [1.25 \pm 0.21] \times 10^6\ M^{-1}$) (Table 1). Upon further addition of PPi, this 2:1 complex rearranges into a 1:1 complex. This is seen from the NMR titration, DOSY spectra, and ESI-MS at higher concentrations of PPi ([PPi]>14 eq.), (Figures S39, S40, and S43).

Here, the fluorescence titration experiments also confirmed the expected analyte-specific spectral response of sensor **3** to various anions, both the fluorescence intensity and the changes in spectral shapes. Thus, the self-quenching is diminished, and the intensity is increased as a result of the changes in conformation and/or expanding the macrocycle due to the binding of various guest (analyte) sizes. The analyte-induced change in spectral shapes is then due to the environmentally sensitive nature of the fluorescent label that translates subtle electronic effects into changes in emission maxima and/or spectral width.[57–59] The combination of both effects is then leveraged as a source of variance in the multivariate analysis described below and allows for the differentiation between the analytes.

Further, we wanted to illustrate the potential practical utility of sensor **3** for sensing of anions in water. In the previous titration experiments, sensor **3** was used in the form of DMSO solution, and the anions were added as a solution in water.

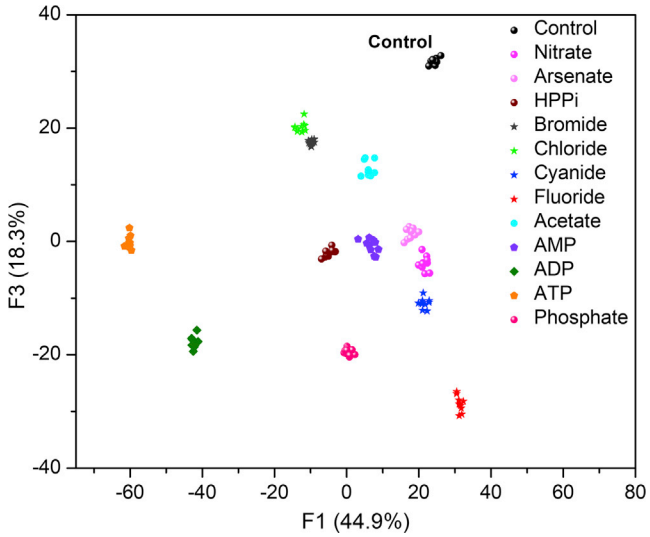

Figure 6. Result of qualitative linear discriminant analysis (LDA)
2D graphical output of the qualitative LDA displaying clusters of 12 analytes and 1 control.

Importantly, the sensor was not hydrolyzed. Due to the lack of solubility of **3** in pure water, a microchip array sensing experiment has been designed utilizing **3** embedded in the hydrophilic polyurethane.[82] Owing to its dual hydrophilic and hydrophobic nature, the polymer accommodates the sensor but also absorbs the water solution while helping to internalize the anions allowing recognition process to take place. The polyurethane-sensor material was applied on a glass microtiter plate (volume of the wells is 500 nL), followed by addition of anion analytes as aqueous solution (200 nL). Distinctive fluorescence output from each well was recorded, and the extracted data were evaluated using linear discriminant analysis (LDA).[6,15,83]

LDA is a statistical method that is maximizing the discriminatory power between different multidimensional data while minimizing the difference within the individual classes to accomplish simpler interpretation of the observed processes (change in fluorescence). The sensor **3** yields an analyte-specific fluorescence response for each studied anion, which enables unambiguous identification of analytes and their concentrations. Figure 6 shows the results of LDA applied to the anion-induced changes in fluorescence of **3**. Here, 13 analytes (12 anions and a control, each in 10 replicas) were correctly classified (Figures S57 and S58). The combination of the flexibility of the sensor macrocycle and the presence of dansyl as an environmentally sensitive fluorophore is believed to be driving the discrimination capability of sensor 3, making it capable of differentiate between multiple analytes.

To further prove the ability of sensor 3 to analyze phosphate anions, we focused on demonstrating the quantitative determination of a biologically important species involved in hydrolysis of ATP to ADP and Pi. As can be seen from the qualitative LDA (Figure 6), ATP, ADP, and phosphate clusters were separated from each other (and the control), suggesting that a quantitative determination of concentrations of ATP/ADP/Pi should be possible. Thus, quantitative LDA analysis for simultaneous determination of ATP, ADP, and $H_2PO_4^-$ was performed (Figure 7A). The quantitative LDA of the ATP, ADP, and Pi shows that each concentration of the anion gives a distinctive cluster corresponding to the analyte type and its concentration. A clear isotherm-like evolution of each analyte and their corresponding clusters in their

Please cite this article in press as: Radujević et al., Cross-reactive binding versus selective phosphate sensing in an imine macrocycle sensor, Chem (2022), https://doi.org/10.1016/j.chempr.2022.05.010

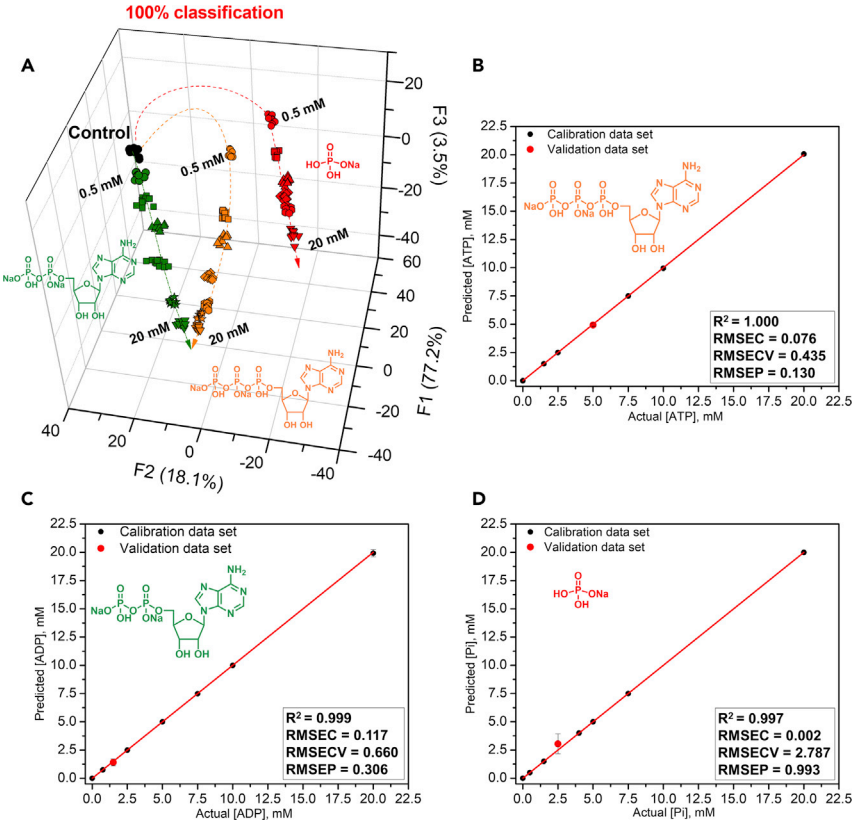

Figure 7. Results of quantitative LDA for ATP, ADP, and Pi

(A–D) (A) 3D graphical output of qualitative LDA for ATP, ADP, and Pi. Quantitative linear regression analysis of the ATP (B), ADP (C), and Pi (D) using support vector machine (SVM) algorithm. The plots of predicted versus actual concentrations of the analytes display high accuracy of the prediction. Root-mean-square errors (RMSEs) of calibration (C), cross-validation (CV), and prediction (P) validate the quality of the model and prediction.

(B–D) Error bars for each data point are associated with the variation of the corresponding values calculated from 10 independent repetitions.

concentration-dependent trends can be seen going from the lowest to the highest concentration. This confirms that the sensor **3** can differentiate between the concentrations of the phosphate analytes, a feature that may be leveraged in further analyses of biologically relevant phosphates.

Here, the smooth trend indicating a predictable behavior of the data in the LDA suggested sensor 3 could be used in quantitative analyses of the phosphates, for example, ATP, ADP, and Pi. Thus, linear regression analysis utilizing support vector machine (SVM)[84,85] was used to perform the quantitative analysis. SVM is a supervised classification method based on mapping the response data into an n-dimensional space utilizing kernel functions. The SVM regression develops calibration models to predict the behavior of the data corresponding to the unknown concentrations of the phosphates. Employing the microtitrations array-like assay using sensor 3, we were able to predict the unknown concentration of the phosphates (ATP, ADP, and Pi). The calculated root-mean-square error for prediction (RMSEP) was < 5% (Figures 7B–7D).

To further demonstrate the potential of this sensor, we explored the sensing of phosphate mixtures. First, we considered a hydrolysis of ATP to AMP and Ppi, then a

Please cite this article in press as: Radujević et al., Cross-reactive binding versus selective phosphate sensing in an imine macrocycle sensor, Chem (2022), https://doi.org/10.1016/j.chempr.2022.05.010

hydrolysis of ATP to ADP and Pi. Toward this end, we have performed a series of high-throughput experiments where the concentrations of ATP were decreasing while the concentrations of AMP and Ppi or ADP and Ppi were increased. In both cases, three different phosphates were present in the mixture, and the sensor yielded unique fluorescence signal for every mixture. Once again, the recorded fluorescence was analyzed by LDA (Figures 8A and S60; Table S4) and followed by linear regression analysis utilizing SVM (Figures 8B and 8C). The LDA shows two clearly identifiable trends for one reaction and a different trend for the other. This is because the analyte constituents are different (ATP/AMP/PPi versus ATP/ADP/Pi) and the sensor **3** displays different affinities and different responses to these anions. Similarly, the SVM regression model shows excellent predictive capabilities (i.e., low error for prediction of unknown concentration, RMSEP, <3.5% for all analytes in the mixture).

Conclusion

To prove our hypothesis that multiple difficult to analyze analytes can be classified and quantified by essentially single sensor molecule comprising a highly cross-reactive receptor and an environmentally sensitive fluorophore capable of converting the binding information into an analyte-specific response, we have prepared a fluorescent imine-oligopyrrole macrocycle **3** that shows conformational flexibility and ability to adjust the size of the binding cavity to accommodate oxo-anions of different size and charge, leveraging the synergy between the hydrogen-donor (pyrrolic **NH**) and hydrogen-acceptor functionalities (imine -**C=N**). NMR and fluorescence studies were performed to explain the folding and unfolding of the macrocycle in response to the anions and provide rationale for why this one-size-fits-all macrocycle can bind mono-, di-, and triphosphates. Importantly, the utility of **3** as a potential sensor for anions is augmented by the notable fluorescence enhancement in the presence of a bound analyte. Thus, **3** displays an interesting interplay between cross-reactivity of the receptor and selectivity in the signal transduction that allows for differentiating even structurally similar anions (cf. $HAsO_4^{2-}$ and $H_2PO_4^-$). The trend of anion affinities is as follows: $HAsO_4^{2-}$ > $H_2PO_4^-$ > AMP > $H_2P_2O_7^{2-}$ > ADP > ATP. To test the practical potential of sensor **3**, an array-like fluorescence sensing of anions using the hydrophilic polyurethane microchip platform was used. On the qualitative level, the polymer-3 chips were used to differentiate between 12 different anions (100% correct classification). Further, we demonstrated the quantitative determination of biologically important species involved in hydrolysis of ATP to ADP and Pi. By applying machine learning algorithms (LDA and SVM), we were able to accurately quantify ATP, ADP, and Pi. Furthermore, the analyses of the ternary mixtures of phosphates that correspond to hydrolyses of ATP (ATP/AMP/PPi and ATP/ADP/Pi mixtures) showed that sensor **3** can distinguish between three different phosphates. This study supports our hypothesis that the concept of combination of a cross-reactive receptor and environmentally sensitive fluorophore enables extracting analyte-specific information in a single sensor molecule, a feature that may be utilized in the design of optimized differential sensor arrays and provide a platform for a practical sensing of environmentally and biologically important phosphorus anions in the near future.

EXPERIMENTAL PROCEDURES

Resource availability

Lead contact

Further information and requests for resources should be directed to and will be fulfilled by the lead contact, Pavel Anzenbacher, Jr. (pavel@bgsu.edu).

Please cite this article in press as: Radujević et al., Cross-reactive binding versus selective phosphate sensing in an imine macrocycle sensor, Chem (2022), https://doi.org/10.1016/j.chempr.2022.05.010

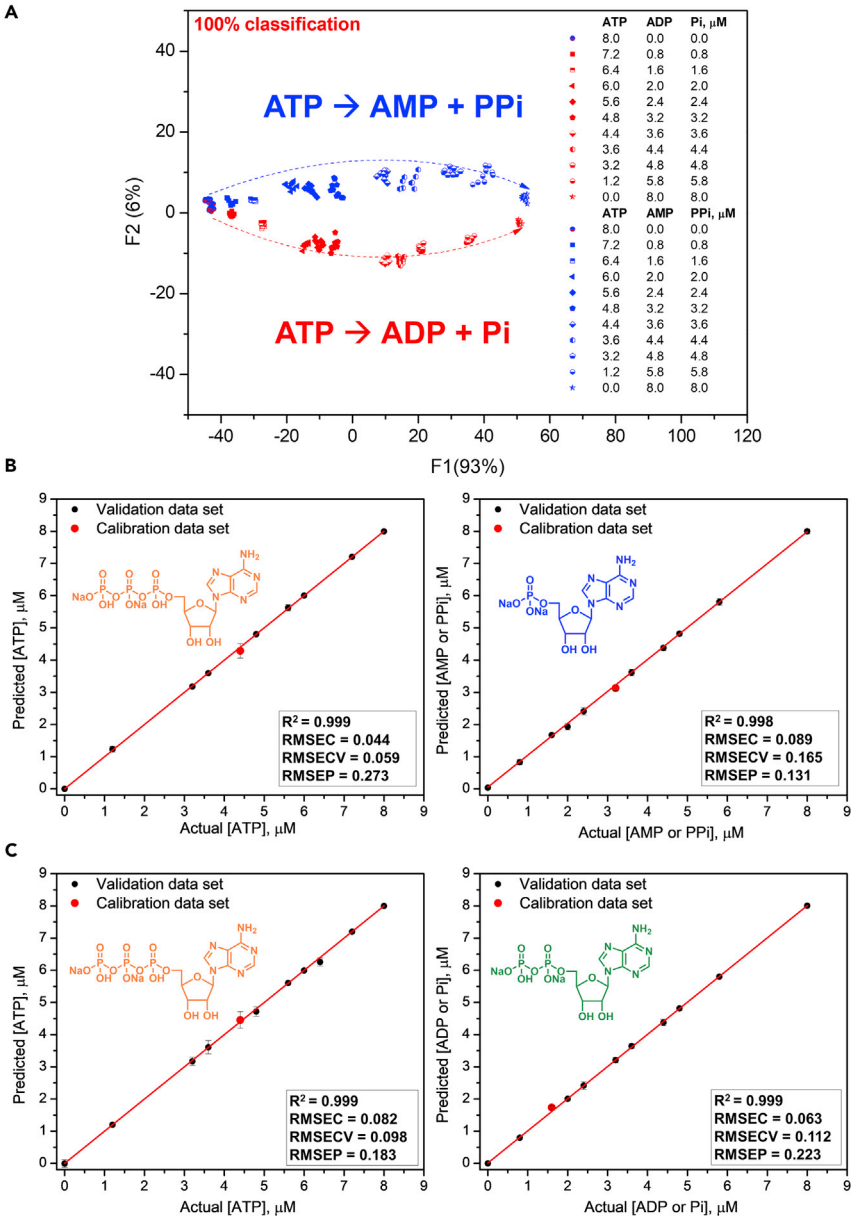

Figure 8. Results of quantitative analysis for ternary mixtures corresponding to ATP hydrolysis (ATP→AMP+PPi and ATP→ADP+Pi)

(A–C) (A) Graphical output of quantitative LDA for various proportions of ATP/AMP/PPi (blue) and ATP/ADP/Pi, (B) quantitative linear regression analysis of the concentration of ATP and AMP, and (C) ATP and ADP using support vector machine (SVM) algorithm. The plots of predicted versus actual concentrations of the analytes display high accuracy of the prediction. Root-mean-square errors (RMSEs) of calibration (C), cross-validation (CV), and prediction (P) validate the quality of the model and prediction.

(B and C) Error bars for each data point are associated with the variation of the corresponding values calculated from 10 independent repetitions.

Materials availability

This study did not generate new unique reagents.

Data and code availability

This study did not generate any datasets.

SUPPLEMENTAL INFORMATION

Supplemental information can be found online at https://doi.org/10.1016/j.chempr.2022.05.010.

ACKNOWLEDGMENTS

We thank Tyler J. Finnegan for assistance in molecular modeling. This work was supported by the National Science Foundation (NSF CHE-2102581 to P.A.), (NSF CHE-2002781 to J.D.B) and Bowling Green State University (Building Strength Award, project no. 33000211 to P.A.). We are grateful to the Ohio Supercomputer Center for allocations of computational resources.

AUTHOR CONTRIBUTIONS

Conceptualization, P.A. and A.R.; methodology, P.A., A.R., and A.P.; formal analysis, A.R. and A.P.; investigation, A.R., A.P., and R.Z.P.; writing – original draft, P.A. and A.R.; writing – review & editing, P.A., A.R., A.P., J.D.B., and R.Z.P.; funding acquisition, P.A. and J.D.B.

DECLARATION OF INTERESTS

The authors declare no competing interests.

Received: December 15, 2021
Revised: January 24, 2022
Accepted: May 12, 2022
Published: June 8, 2022

REFERENCES

1. Behr, J.P. (2008). The Lock-and-Key Principle: the State of the Art–100 Years on (Wiley).

2. Peveler, W.J., Yazdani, M., and Rotello, V.M. (2016). Selectivity and specificity: pros and cons in sensing. ACS Sens *1*, 1282–1285.

3. Lavigne, J.J., and Anslyn, E.V. (2001). Sensing A paradigm shift in the field of molecular recognition: From selective to differential receptors. Angew. Chem. Int. Ed. Engl. *40*, 3118–3130.

4. Albert, K.J., Lewis, N.S., Schauer, C.L., Sotzing, G.A., Stitzel, S.E., Vaid, T.P., and Walt, D.R. (2000). Cross-reactive chemical sensor arrays. Chem. Rev. *100*, 2595–2626.

5. Hamedpour, V., Sasaki, Y., Zhang, Z., Kubota, R., and Minami, T. (2019). Simple colorimetric chemosensor array for oxyanions: quantitative assay for herbicide glyphosate. Anal. Chem. *91*, 13627–13632.

6. Mitchell, L., New, E.J., and Mahon, C.S. (2021). Macromolecular optical sensor arrays. ACS Appl. Polym. Mater. *3*, 506–530.

7. Li, Z., Askim, J.R., and Suslick, K.S. (2019). The optoelectronic nose: colorimetric and fluorometric sensor arrays. Chem. Rev. *119*, 231–292.

8. Geng, Y., Peveler, W.J., and Rotello, V.M. (2019). Array-based "chemical nose" sensing in diagnostics and drug discovery. Angew. Chem. Int. Ed. Engl. *58*, 5190–5200.

9. Stitzel, S.E., Aernecke, M.J., and Walt, D.R. (2011). Artificial noses. Annu. Rev. Biomed. Eng. *13*, 1–25.

10. Freudenberg, J., Hinkel, F., Jänsch, D., and Bunz, U.H.F. (2018). Chemical tongues and noses based upon conjugated polymers. In Polymer Synthesis Based on Triple-Bond Building Blocks, B.Z. Tang and R. Hu, eds. (Springer International Publishing), pp. 191–239.

11. Chen, Z.-H., Fan, Q.-X., Han, X.-Y., Shi, G., and Zhang, M. (2020). Design of smart chemical 'tongue' sensor arrays for pattern-recognition-based biochemical sensing applications. Trends Anal. Chem. *124*, 115794.

12. Wang, Q.Q., Fang, Z.Q., Wu, Y.T., Zhang, M., and Shi, G. (2020). A single-component yet multifunctional tongue-mimicking sensor array for upconversion fluorescence biosensing. Analyst *145*, 7191–7196.

13. Sugai, H., Tomita, S., and Kurita, R. (2020). Pattern-recognition-based sensor arrays for cell characterization: From materials and data analyses to biomedical applications. Anal. Sci. *36*, 923–934.

14. Diehl, K.L., and Anslyn, E.V. (2013). Array sensing using optical methods for detection of chemical and biological hazards. Chem. Soc. Rev. *42*, 8596–8611.

15. Anzenbacher, P., Jr., Lubal, P., Buček, P., Palacios, M.A., and Kozelkova, M.E. (2010). A practical approach to optical cross-reactive sensor arrays. Chem. Soc. Rev. *39*, 3954–3979.

16. Wright, A.T., and Anslyn, E.V. (2006). Differential receptor arrays and assays for solution-based molecular recognition. Chem. Soc. Rev. *35*, 14–28.

17. Inouye, M., Hashimoto, K., and Isagawa, K. (1994). Nondestructive detection of acetylcholine in Protic media: artificial-signaling acetylcholine receptors. J. Am. Chem. Soc. *116*, 5517–5518.

18. Wang, B., Han, J., Bojanowski, N.M., Bender, M., Ma, C., Seehafer, K., Herrmann, A., and Bunz, U.H.F. (2018). An optimized sensor array identifies all natural amino acids. ACS Sens *3*, 1562–1568.

19. Chen, R.R., Luo, D.H., Sun, Y., Sun, Y.L., and Gholam Hossini, H. (2014). A sensor array optimization method based on variance difference for machine olfaction. Appl. Mech. Mater. *618*, 523–527.

20. Palacios, M.A., Wang, Z., Montes, V.A., Zyryanov, G.V., and Anzenbacher, P. (2008). Rational design of a minimal size sensor array for metal ion detection. J. Am. Chem. Soc. *130*, 10307–10314.

21. Liu, Y., Minami, T., Nishiyabu, R., Wang, Z., and Anzenbacher, P. (2013). Sensing of carboxylate drugs in urine by a supramolecular sensor array. J. Am. Chem. Soc. *135*, 7705–7712.

22. Sasaki, Y., Lyu, X., Zhang, Z., and Minami, T. (2022). A minimized fluorescent chemosensor array utilizing carboxylate-attached polythiophenes on a chip for metal ions detection. Front. Chem. Sci. Eng. *16*, 72–80.

23. Demchenko, A.P. (2005). The future of fluorescence sensor arrays. Trends Biotechnol *23*, 456–460.

24. Pushina, M., Penavic, A., Farshbaf, S., and Anzenbacher, P. (2021). Fluorescent sensor array for quantitative determination of saccharides. ACS Sens *6*, 4001–4008.

25. Rana, S., Elci, S.G., Mout, R., Singla, A.K., Yazdani, M., Bender, M., Bajaj, A., Saha, K., Bunz, U.H.F., Jirik, F.R., and Rotello, V.M. (2016). Ratiometric array of conjugated polymers–fluorescent protein provides a robust mammalian cell sensor. J. Am. Chem. Soc. *138*, 4522–4529.

26. Pushina, M., Farshbaf, S., Shcherbakova, E.G., and Anzenbacher, P. (2019). A dual chromophore sensor for the detection of amines, diols, hydroxy acids, and amino alcohols. Chem. Commun. (Camb) *55*, 4495–4498.

27. Sothivelr, K., Bender, F., Josse, F., Yaz, E.E., and Ricco, A.J. (2019). Quantitative detection of complex mixtures using a single chemical sensor: analysis of response transients using multi-stage estimation. ACS Sens *4*, 1682–1690.

28. Dziuba, D., Postupalenko, V.Y., Spadafora, M., Klymchenko, A.S., Guérineau, V., Mély, Y., Benhida, R., and Burger, A. (2012). A universal nucleoside with strong two-band switchable fluorescence and sensitivity to the environment for investigating DNA interactions. J. Am. Chem. Soc. *134*, 10209–10213.

29. Sasaki, Y., Kojima, S., Hamedpour, V., Kubota, R., Takizawa, S., Yoshikawa, I., Houjou, H., Kubo, Y., and Minami, T. (2020). Accurate chiral pattern recognition for amines from just a single chemosensor. Chem. Sci. *11*, 3790–3796.

30. Jarvie, H.P., Sharpley, A.N., Flaten, D., Kleinman, P.J.A., Jenkins, A., and Simmons, T. (2015). The pivotal role of phosphorus in a resilient water–energy–food security nexus. J. Environ. Qual. *44*, 1049–1062.

31. Hirsch, A.K.H., Fischer, F.R., and Diederich, F. (2007). Phosphate recognition in structural biology. Angew. Chem. Int. Ed. Engl. *46*, 338–352.

32. Cordell, D., Drangert, J.-O., and White, S. (2009). The story of phosphorus: global food security and food for thought. Glob. Environ. Change *19*, 292–305.

33. Kleinman, P.J.A., Sharpley, A.N., McDowell, R.W., Flaten, D.N., Buda, A.R., Tao, L., Bergstrom, L., and Zhu, Q. (2011). Managing agricultural phosphorus for water quality protection: principles for progress. Plant Soil *349*, 169–182.

34. Murphy, J., and Riley, J.P. (1962). A modified single solution method for the determination of phosphate in natural waters. Anal. Chim. Acta *27*, 31–36.

35. Van Veldhoven, P.P., and Mannaerts, G.P. (1987). Inorganic and organic phosphate measurements in the nanomolar range. Anal. Biochem. *161*, 45–48.

36. Wei, H., Pan, D., Zhou, Z., Han, H., and Zhu, R. (2021). On-site electrochemical determination of phosphate with high sensitivity and anti-interference ability in turbid coastal waters. Ecotoxicol. Environ. Saf. *221*, 112444.

37. Barhoumi, L., Baraket, A., Nooredeen, N.M., Ali, M.B., Abbas, M.N., Bausells, J., and Errachid, A. (2017). Silicon nitride capacitive chemical sensor for phosphate ion detection based on copper phthalocyanine – acrylate-polymer. Electroanalysis *29*, 1586–1595.

38. Bhat, K.S., Nakate, U.T., Yoo, J.Y., Wang, Y., Mahmoudi, T., and Hahn, Y.B. (2019). Nozzle-jet-printed silver/graphene composite-based field-effect transistor sensor for phosphate ion detection. ACS Omega *4*, 8373–8380.

39. Zhou, G., Jin, B., Wang, Y., Dong, Q., Maity, A., Chang, J., Ren, R., Pu, H., Sui, X., Mao, S., et al. (2020). Ultrasensitive sensors based on aluminum oxide-protected reduced graphene oxide for phosphate ion detection in real water. Mol. Syst. Des. Eng. *5*, 936–942.

40. Fabbro, D., Cowan-Jacob, S.W., and Moebitz, H. (2015). Ten things you should know about protein kinases: IUPHAR Review 14. Br. J. Pharmacol. *172*, 2675–2700.

41. Svoboda, L., and Schmidt, U. (1997). Single-column ion chromatography of linear polyphosphates. J. Chromatogr. A *767*, 107–113.

42. Juarez-Facio, A.T., Martin de Lagarde, V., Monteil, C., Vaugeois, J.M., Corbiere, C., and Rogez-Florent, T. (2021). Validation of a fast and simple HPLC-UV method for the quantification of adenosine phosphates in human bronchial epithelial cells. Molecules *26*.

43. Menegollo, M., Tessari, I., Bubacco, L., and Szabadkai, G. (2019). Determination of ATP, ADP, and AMP levels by reversed-phase high-performance liquid chromatography in cultured cells. In Calcium Signalling: Methods and Protocols, A. Raffaello and D. Vecellio Reane, eds. (Springer), pp. 223–232.

44. Hargrove, A.E., Nieto, S., Zhang, T., Sessler, J.L., and Anslyn, E.V. (2011). Artificial receptors for the recognition of phosphorylated molecules. Chem. Rev. *111*, 6603–6782.

45. Pal, S., Ghosh, T.K., Ghosh, R., Mondal, S., and Ghosh, P. (2020). Recent advances in recognition, sensing and extraction of phosphates: 2015 onwards. Coord. Chem. Rev. *405*, 213128.

46. Ramakrishnam Raju, M.V., Harris, S.M., and Pierre, V.C. (2020). Design and applications of metal-based molecular receptors and probes for inorganic phosphate. Chem. Soc. Rev. *49*, 1090–1108.

47. Hofmeister, F. (1888). Zur Lehre von der Wirkung der Salze. Archiv f. experiment. Pathol. u. Pharmakol. *24*, 247–260.

48. Beer, P.D., and Gale, P.A. (2001). Anion recognition and sensing: the state of the art and future perspectives. Angew. Chem. Int. Ed. Engl. *40*, 486–516.

49. Sessler, J.L., Gale, P., Cho, W.-S., Stoddart, J.F., Rowan, S.J., Aida, T., and Rowan, A.E. (2006). Anion Receptor Chemistry (The Royal Society of Chemistry).

50. Ojida, A., Miyahara, Y., Wongkongkatep, J., Tamaru, S., Sada, K., and Hamachi, I. (2006). Design of dual-emission chemosensors for ratiometric detection of ATP derivatives. Chem. Asian J. *1*, 555–563.

51. Mailhot, R., Traviss-Pollard, T., Pal, R., and Butler, S.J. (2018). Cationic europium complexes for visualizing fluctuations in mitochondrial ATP levels in living cells. Chemistry *24*, 10745–10755.

52. Huston, M.E., Akkaya, E.U., and Czarnik, A.W. (1989). Chelation enhanced fluorescence detection of non-metal ions. J. Am. Chem. Soc. *111*, 8735–8737.

53. Goshisht, M.K., and Tripathi, N. (2021). Fluorescence-based sensors as an emerging tool for anion detection: mechanism, sensory materials and applications. J. Mater. Chem. C *9*, 9820–9850.

54. Busschaert, N., Caltagirone, C., Van Rossom, W., and Gale, P.A. (2015). Applications of supramolecular anion recognition. Chem. Rev. *115*, 8038–8155.

55. Tay, H.M., and Beer, P. (2021). Optical sensing of anions by macrocyclic and interlocked hosts. Org. Biomol. Chem. *19*, 4652–4677.

56. Lum, K., Zielinski, S.M., and Abelt, C.J. (2021). Dansyl emits from a PICT excited state. J. Phys. Chem. A *125*, 1229–1233.

57. Klymchenko, A.S. (2017). Solvatochromic and fluorogenic dyes as environment-sensitive probes: design and biological applications. Acc. Chem. Res. *50*, 366–375.

58. Shvadchak, V.V., Kucherak, O., Afitska, K., Dziuba, D., and Yushchenko, D.A. (2017). Environmentally sensitive probes for monitoring protein-membrane interactions at nanomolar concentrations. Biochim. Biophys. Acta Biomembr. *1859*, 852–859.

59. Esipenko, N.A., Koutnik, P., Minami, T., Mosca, L., Lynch, V.M., Zyryanov, G.V., and Anzenbacher, P. (2013). First supramolecular sensors for phosphonate anions. Chem. Sci. *4*, 3617–3623.

60. Pavlović, R.Z., Lalisse, R.F., Hansen, A.L., Waudby, C.A., Lei, Z., Güney, M., Wang, X., Hadad, C.M., and Badjić, J.D. (2021). From selection to instruction and back: competing conformational selection and induced fit pathways in abiotic Hosts. Angew. Chem. Int. Ed. Engl. *60*, 19942–19948.

61. Hong, C.M., Kaphan, D.M., Bergman, R.G., Raymond, K.N., and Toste, F.D. (2017). Conformational selection as the mechanism of guest binding in a flexible supramolecular Host. J. Am. Chem. Soc. *139*, 8013–8021.

62. Yang, L.P., Zhang, L., Quan, M., Ward, J.S., Ma, Y.L., Zhou, H., Rissanen, K., and Jiang, W. (2020). A supramolecular system that strictly follows the binding mechanism of conformational selection. Nat. Commun. *11*, 2740.

63. Bianchi, A., Bowman-James, K., and García-España, E. (2011). Aspects of anion coordination from historical perspectives. In Anion Coordination Chemistry (John Wiley & Sons, Ltd), pp. 1–73.

64. Callaway, W.B., Veauthier, J.M., and Sessler, J.L. (2004). Schiff-base porphyrin and expanded porphyrin analogs. J. Porphyrins Phthalocyanines *08*, 1–25.

65. Sessler, J.L., and Weghorn, S.J. (1997). Expanded, Contracted & Isomeric Porphyrins (Pergamon).

66. Borisova, N.E., Reshetova, M.D., and Ustynyuk, Y.A. (2007). Metal-free methods in the synthesis of macrocyclic Schiff bases. Chem. Rev. *107*, 46–79.

67. Katayev, E.A., Boev, N.V., Khrustalev, V.N., Ustynyuk, Y.A., Tananaev, I.G., and Sessler, J.L. (2007). Bipyrrole- and Dipyrromethane-based amido-imine hybrid macrocycles. New receptors for oxoanions. J. Org. Chem. *72*, 2886–2896.

68. Katayev, E.A., Pantos, G.D., Lynch, V.M., Sessler, J.L., Reshetova, M.D., and Ustynyuk, Yu.A. (2005). New polydentate macrocyclic ligands of hybrid amine-imine and amide-imine types as artificial anion receptors. Synthesis and study of anion binding. Russ. Chem. Bull. *54*, 165–172.

69. Kolesnikov, G.V., German, K.E., Kirakosyan, G., Tananaev, I.G., Ustynyuk, Y.A., Khrustalev, V.N., and Katayev, E.A. (2011). Macrocyclic receptor for pertechnetate and perrhenate anions. Org. Biomol. Chem. *9*, 7358–7364.

70. Katayev, E.A., Sessler, J.L., Khrustalev, V.N., and Ustynyuk, Y.A. (2007). Synthetic model of the phosphate binding protein: solid-state structure and solution-phase anion binding properties of a large Oligopyrrolic macrocycle. J. Org. Chem. *72*, 7244–7252.

71. Oh, J.H., Kim, J.H., Kim, D.S., Han, H.J., Lynch, V.M., Sessler, J.L., and Kim, S.K. (2019). Synthesis and anion recognition features of a molecular cage containing both hydrogen bond donors and acceptors. Org. Lett. *21*, 4336–4339.

72. Xie, H., Finnegan, T.J., Liyana Gunawardana, V.W., Pavlović, R.Z., Moore, C.E., and Badjić, J.D. (2021). A hexapodal capsule for the recognition of anions. J. Am. Chem. Soc. *143*, 3874–3880.

73. Han, H.J., Oh, J.H., Sessler, J.L., and Kim, S.K. (2019). Small triiminopyrrolic molecular cage with high affinity and selectivity for fluoride. Chem. Commun. (Camb) *55*, 10876–10879.

74. Mahanta, S.P., Kumar, B.S., Baskaran, S., Sivasankar, C., and Panda, P.K. (2012). Colorimetric sensing of fluoride ion by new expanded calix[4]pyrrole through anion–π interaction. Org. Lett. *14*, 548–551.

75. Upendar Reddy, G., Lo, R., Roy, S., Banerjee, T., Ganguly, B., and Das, A. (2013). A new receptor with a FRET based fluorescence response for selective recognition of fumaric and maleic acids in aqueous medium. Chem. Commun. *49*, 9818–9820.

76. Release, S. (2017). MacroModel (Schrödinger, LLC), pp. 2021–2022.

77. Release, S. (2017). Maestro (Schrödinger, LLC), pp. 2021–2022.

78. Harder, E., Damm, W., Maple, J., Wu, C., Reboul, M., Xiang, J.Y., Wang, L., Lupyan, D., Dahlgren, M.K., Knight, J.L., et al. (2016). OPLS3: A force field providing broad coverage of drug-like small molecules and proteins. J. Chem. Theory Comput. *12*, 281–296.

79. Zyryanov, G.V., Palacios, M.A., and Anzenbacher, P., Jr. (2007). Rational design of a fluorescence-turn-on sensor array for phosphates in blood serum. Angew. Chem. Int. Ed. Engl. *46*, 7849–7852.

80. Thordarson, P. (2011). Determining association constants from titration experiments in supramolecular chemistry. Chem. Soc. Rev. *40*, 1305–1323.

81. Ulatowski, F., Dąbrowa, K., Bałakier, T., and Jurczak, J. (2016). Recognizing the limited applicability of job plots in studying Host-Guest Interactions in Supramolecular Chemistry. J. Org. Chem. *81*, 1746–1756.

82. Anzenbacher, P., Jr., Liu, Y., Palacios, M.A., Minami, T., Wang, Z., and Nishiyabu, R. (2013). Leveraging material properties in fluorescence anion sensor arrays: A general approach. Chemistry *19*, 8497–8506.

83. Shcherbakova, E.G., Minami, T., Brega, V., James, T.D., and Anzenbacher, P., Jr. (2015). Determination of enantiomeric excess in amine derivatives with molecular self-assemblies. Angew. Chem. Int. Ed. Engl. *54*, 7130–7133.

84. Hamel, L. (2009). Knowledge Discovery with Support Vector Machines (Wiley).

85. Cristianini, N., and Shawe-Taylor, J. (2000). An Introduction to Support Vector Machines and Other Kernel-Based Learning Methods (Cambridge University Press).